Research paper

Mid- and late-Holocene sedimentary process and palaeovegetation changes near the mouth of the Amazon River

The Holocene
22(3) 359–370

DOI: 10.1177/0959683611423693
hol.sagepub.com
SAGE

José Tasso Felix Guimarães,[1] Marcelo Cancela Lisboa Cohen,[1] Luiz Carlos Ruiz Pessenda,[2] Marlon Carlos França,[1] Clarisse Beltrão Smith[1] and Afonso César Rodrigues Nogueira[1]

Abstract

The integration of sedimentary facies, pollen, spores, carbon and nitrogen isotopes records, C/N ratio and radiocarbon dates allowed the identification of changes in vegetation and the sources of organic matter accumulated on tidal flats near the mouth of the Amazon River during the mid and late Holocene. Data from the margin of Amazon River indicate marine influence related to mangrove presence over a tidal mud flat between 5560–5470 cal. yr BP and 5290–5150 cal. yr BP. Afterward, the mangrove area shrank following the return of more humid conditions and increase of Amazon River discharge. A common reworking process of the tidal flat through the lateral migration of a meandering creek occurred in the study site, with later development of transitional vegetation under freshwater influence. Following the natural vegetation succession under stable climate and hydrological conditions, the expansion of 'várzea' (flooded freshwater vegetation) forests occurred since 600–560 cal. yr BP until the present. Furthermore, regarding the tidal flats located west of the mouth of Amazon River, these stable conditions also allowed the mangrove maintenance over mudflats with deposition of marine organic matter during at least the last 2350–2300 cal. yr BP.

Keywords

Amazonia, C and N isotopes, climate changes, facies analysis, Holocene, palynology

Introduction

Morphological, climatic and hydrological factors have produced the formation of geobotanical units of the Amazonian coastal region leading to the development of a marine-influenced littoral (southeastern coastline), dominated by mangroves and saltmarsh vegetation, and a fluvial sector (northwestern coastline), characterized by 'várzea' (flooded freshwater forests) and herbaceous vegetation (Cohen et al., 2009).

Palaeoenvironmental research in the marine littoral shows mangrove establishment between 7500 and 5100 cal. yr BP (Behling and Costa, 2001; Behling et al., 2001; Cohen et al., 2005) during the Holocene reflecting the postglacial sea-level rise that invaded the coast embayed by rather shallow and broad valleys (Cohen et al., 2005; Souza Filho et al., 2006), while the fluvial littoral presents tidal flat deposits influenced by marine processes during the Holocene with vegetation history characterized by mangrove and 'várzea' expansion/contraction phases (Cohen et al., 2008; Guimarães et al., 2010).

Toledo and Bush (2007) recorded declining abundance of *Rhizophora* pollen after c. 7000 cal. yr BP, suggesting a weakening of the marine influence and, from 5000 cal. yr BP, the replacement of closed forest elements by open flooded savanna. Those findings indicate reduced discharge from the Amazon River, likely due to a marked decrease in precipitation in the Andes between 8000 and 5000 cal. yr BP.

Several studies indicate that Amazon climate has varied during the Holocene with significant fluctuations in precipitation (e.g. Absy et al., 1991; Behling and Costa, 2000; Desjardins et al., 1996; Ledru, 2001; Pessenda et al., 2001; Van der Hammen, 1974), and possibly, in the river water discharge such as Amazon River and its tributaries (e.g. Latrubesse and Franzinelli, 2002; Maslin and Burns, 2000).

In Amapá littoral, extensive tidal flat deposits developed adjacent to the Amazon River may be more appropriate to investigate vegetation changes related to variations of the Amazon River discharge during the Holocene. However, few palaeoecological studies based on pollen data were performed in this area (Guimarães et al., 2010; Toledo and Bush, 2007).

Considering the techniques applied in this work, the facies analysis is traditionally used to define characteristics of a sedimentary unit that formed under certain hydrodynamic processes and sedimentation environment. Thus, each depositional environment puts its own imprint on the sediment, resulting in a singular facies (e.g. Walker, 1992), while pollen records from vegetated tidal flats tend to represent local vegetation and the strength of the pollen signal from each phytophysiognomy is distance-weighted (e.g. Behling et al., 2004; Cohen et al., 2009; Guimarães et al.,

[1]Universidade Federal do Pará (UFPA), Brazil
[2]Centro de Energia Nuclear na Agricultura (CENA), Brazil

Received 18 March 2011; revised manuscript accepted 22 August 2011

Corresponding author:
José Tasso Felix Guimarães, Programa de Pós-Graduação em Geologia e Geoquímica, Instituto de Geociências, Universidade Federal do Pará (UFPA), Rua Augusto Correa 01, 66075-110, Belém/PA, Brazil.
Email: tasso@ufpa.br

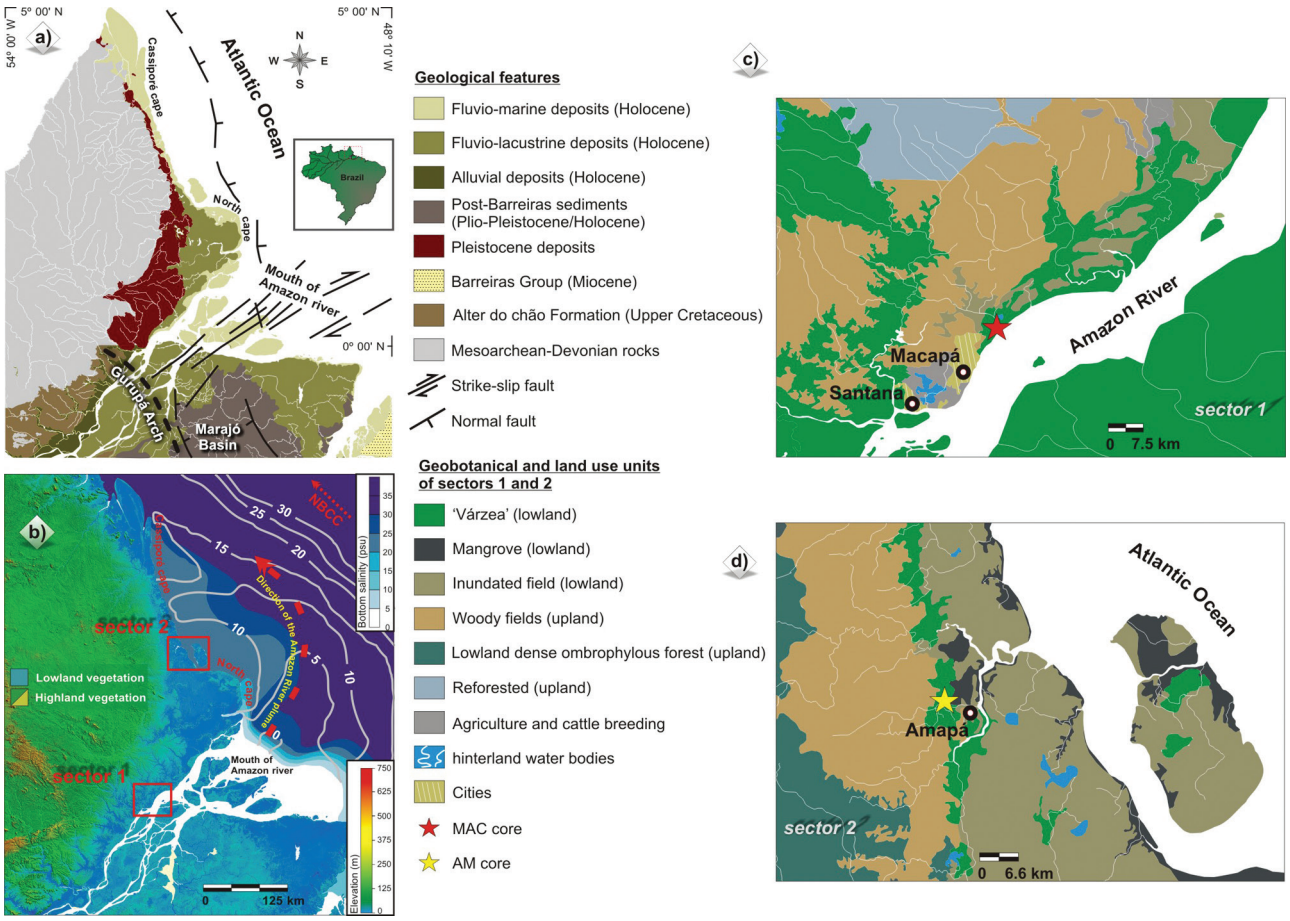

Figure 1. Study site: (a) regional geology of the study area in the Marajó basin (modified from CPRM, 2010 and Costa et al., 2002), (b) elevation map with bottom and surface water salinity, direction of the Amazon River plume and North Brazilian Coastal Current (NBCC) near the Amapá littoral (modified from Vinzon et al., 2008 and Rosario et al., 2009), (c) and (d) geobotanical and land use units of sectors 1 (Macapá) and 2 (Amapá) with sampling sites

2010). As additional information, carbon and nitrogen isotope ($\delta^{13}C$ and $\delta^{15}N$) and carbon to nitrogen ratios (C/N) can be used, since they can provide data about the origin of organic matter (e.g. Lamb et al., 2006).

Thus, an interdisciplinary approach based on facies analysis, isotopic and pollen records may provide better information about process and environment of deposition, and the origin of organic matter preserved in coastal deposits, respectively (Dalrymple and Choi, 2007; Lamb et al., 2006), which is required to isolate the climatic signal from the non-climatic noise and better interpret the main process acting on coastal systems as indications of hydrodynamic regime, river discharge, organic matter sources and vegetation patterns (e.g. Engelhart et al., 2007; Freycon et al., 2009; Horton et al., 2005). This interproxy study was applied in order to investigate the sedimentary process, vegetation changes and sources of organic matter accumulated on tidal flats near the mouth of Amazon River during the mid and late Holocene.

Study area

Geological and physiographic setting

The coastal zone of Amapá in the study area is located in the Marajó basin that is linked to the Gondwana break up and Equatorial Atlantic opening during Jurassic/early Cretaceous (Szatmari et al., 1987). This basin is limited to the south and west by Gurupá and Tocantins arches, respectively.

The regional geology includes Mesoarchean-Devonian Crystalline and Metassedimentary rocks to the western part, and Pleistocene sandstone and conglomerates in the eastern part interpreted as tidal depositional systems (Souza and Pinheiro, 2009). From the Late Pleistocene to Holocene, erosional and depositional processes due to Late Pleistocene and Holocene climatic and sea-level changes, along with tectonic processes, shaped the relief of the Amapá coast, resulting in its current configuration (Lima et al., 1991). Therefore, along the coastal plain adjacent to the Amazon River, extensive north–south trending Holocene terraces composed of sand and mud have developed (Figure 1a, b). The very flat, low-elevation landscape is characterized by flooded areas and both abandoned and active meandering channels (Figure 1b). The coast between Cassiporé and North Cape, which is part of the longest muddy coastline in the world (Figure 1a, b), is strongly influenced by Amazon River discharge (Allison et al., 2000).

Floristic studies of Costa Neto (2004), Costa Neto and Silva (2004), Carvalho et al. (2006) and Costa Neto et al. (2007) described geobotanical and land-use units (Figure 1c, d). For sectors 1 (freshwater influence) and 2 (brackish water influence) (Figure 1c, d and Table 1), a vegetation survey based on qualitative descriptions was carried out. The modern vegetation of Macapá region – sector 1 (Figure 1c) is represented by periodically inundated herbaceous-shrubs field (upland to supratidal zone) and permanently inundated herbaceous field (supratidal zone). The supratidal and intertidal zone are colonized by well-developed 'várzea' (flooded freshwater forests). The vegetation of Amapá region – sector 2 (Figure 1d) is characterized by well-developed mangrove forests near the coastline, herbs vegetation (supratidal zone), and 'várzea'.

Table 1. Main plant species identified in the study site

Family and species	Biological form	Macapá (sec. 1)	Amapá (sec. 2)	Vegetation units
Aizoaceae				
Sesuvium sp.	Herb		X	IF
Anarcadiaceae				
Tapirira sp.	Tree	X	X	VF
Aquifoliaceae				
Ilex sp.	Tree	X		VF
Araceae				
Montrichardia sp.	Herb	X	X	VF
Arecaceae				
Euterpe sp.	Tree	X	X	VF
Mauritia sp.	Tree	X	X	VF
Avicenniaceae				
Avicennia sp.	Tree		X	MG
Cabombaceae				
Cabomba sp.	Herb	X	X	VF, IF
Ceratopteridaceae				
Acrostichum sp	Herb		X	MG
Cobretaceae				
Laguncularia sp.	Tree		X	MG
Cyperaceae				
Cyperus sp.	Herb	X	X	IF
Scleria sp.	Herb	X	X	IF
Euphorbiaceae				
Alchornea sp.	Tree	X	X	VF
Hevea sp.	Tree	X	X	VF
Fabaceae				
Macrolobium sp.	Tree	X	X	VF
Parkia nitida Miq.	Tree	X	X	VF
Helioconiaceae				
Heliconia sp.	Herb	X	X	IF
Malpighiaceae				
Mascagnia sp.	Climber	X	X	FV
Malvaceae				
Pachira sp.	Tree	X	X	VF
Pseudobombax sp.	Tree	X	X	VF
Nymphaeceae				
Nymphaea sp.	Herb	X	X	VF, IF
Poaceae				
Olyra latifolia L.	Herb	X	X	VF, IF
Panicum laxum Sw.	Herb	X	X	IF
Paspalum sp.	Herb	X	X	IF
Ponteridaceae				
Eichhornia sp.	Herb	X	X	IF
Rubiaceae	Herb			
Alibertia sp.	Tree	X	X	FV
Psychotria	Herb	X	X	IF
Rhizophoraceae				
Rhizophora sp.	Tree		X	MG
Strelitziaceae				
Phenakospermum sp.	Herb	X		VF

Vegetation units, VF, Varzea forest; IF, Inundated Field; MG, Mangrove.

Climate and hydrology

The regional climate is humid tropical characterized by well-defined dry (September to December) and wet (January to July) seasons, with annual average precipitation and temperature around 3000 mm and 27.5°C, respectively (Bezerra et al., 1990). The mean Amazon River discharge is about 170 000 m^3/s (at Óbidos city), with maximum and minimum outflow of 270 000 and 60 000 m^3/s (ANA, 2003). The Amazon estuary is classified as semi-diurnal macrotidal (Pugh, 1987), with a tidal range of 4 to 6 m (Gallo and Vinzon, 2005). The structure of the plume is controlled by the North Brazilian Current, which induces a northwestern flow with speeds of 40–80 cm/s over the continental shelf (Figure 1b; Lentz, 1995), strong tidal currents (Beardsley et al., 1995), trade winds and the Intertropical Convergence Zone (ITCZ; Lentz and Limeburner, 1995). Consequently, the river discharge and hydrodynamic conditions allow a strong reduction of water salinity along the Amazon River and adjacent coast (Figure 1b; Rosario et al., 2009; Vinzon et al., 2008).

Table 2. Carbon Isotopic ($\delta^{13}C$) signature of leaves from main genres of the study site showing C3 plant dominance (more depleted values ranging from −26.6 to −34.4)

Family	Species	$\delta^{13}C$ (‰) $_{VPDB}$
Aizoaceae	*Sesuvium* sp.	−13.9
Arecaceae	*Euterpe oleracea* Mart.	−34.4
Araceae	*Montrichardia arborescens* (L.) Schott.	−27.6
	Pistia stratioides L.	−26.6
Avicenniaceae	*Avicennia germinans* (L.) Stearn	−31
Cyperaceae	*Cyperus* sp.	−29.8
Heliconiaceae	*Heliconia* sp.	−29.7
Strelitziaceae	*Phenakospermum* sp.	−34.3
Nymphaeaceae	*Nymphaea* sp.	−27
Poaceae	*Panicum* sp.	−12
	Hymenachne amplexicaule (Rudge) Nees.	−29.2
	Olyra latifolia L.	−32
	Paspalum repens Berg.	−11
Pteridaceae	*Acrostichum* L.	−32
Rhizophoraceae	*Rhizophora mangle L.*	−33.5

Materials and methods

Sampling and facies description

The sediment cores were sampled from the city of Macapá – sector 1 (freshwater influence), and the city of Amapá – sector 2 (brackish water influence) (Figure 1c, d) using a Russian Sampler with the geographical position of each point determined by GPS (Reference Datum: Sad69). Following the proposal of Walker (1992), facies analysis included descriptions of color, lithology, texture and structures. X-ray radiographs aided the identification of sedimentary structures. The sedimentary facies was codified following Miall (1978). The interpretation of the sedimentological data is also based on clastic tidalite process-response models (after Klein, 1971). Leaves of the most abundant genera were collected to heights of up to 2 m, to identify the carbon isotopic signatures (Table 2). Sediment cores were sampled from tidal flats colonized by 'várzea' (sector 1 – MAC core to 2 m depth, 00°04′15″N, 51°02′15″W, ~5–7 m above mean sea level (a.m.s.l.), and 0.3 km from the Amazon River), and mangrove vegetation (sector 2 – AM core to 1 m depth, 02°03′08″N, 50°48′21″W, ~ 2–4 m a.m.s.l., 15 km away from the coastline and 150 km from the mouth of Amazon River).

Pollen and spore analyses

Throughout the sediment cores, 1 cm^3 of sediments were picked in 5 cm intervals. One tablet of exotic *Lycopodium* spores was added to each sample for the calculation of pollen concentration (grains/cm^3). All samples were prepared using standard techniques of pollen analysis including acetolysis (Faegri and Iversen, 1989). Handbooks of pollen and spores morphology were consulted (Colinvaux et al., 1999; Hesse et al., 2008; Roubik and Moreno, 1991) jointly with the reference collection of the 'Laboratório de Dinâmica Costeira – UFPa' to identify of pollen grains and spores. Samples were counted to a minimum of about 300 pollen grains. The total pollen sum only considers pollen grains and excludes algae, microforaminifers, fungal and fern spores. Forty pollen taxa were identified. Pollen and spore data are presented in pollen diagrams as percentages of the total pollen amount. Taxa were grouped into Vegetation units: Mangrove, Inundated field, 'várzea' and Transitional/Secondary Forest (TSF). The software Tilia and Tilia Graph were used for the calculation and plotting of pollen diagrams. The pollen diagrams were statistically subdivided into zones of pollen and spores assemblages based on square-root-transformation of the percentage data and stratigraphically constrained cluster analysis by the method of total sum of squares (Grimm, 1987).

C/N, carbon and nitrogen isotopes

The $\delta^{13}C$, $\delta^{15}N$ and elemental C and N (C/N) amounts were analyzed from sediment samples (6–50 mg) taken at 5 cm intervals along the cores. The stable carbon and nitrogen isotopes as well as the total organic carbon (TOC) and nitrogen (TN) were determined at the Stable Isotopes Laboratory of Center for Nuclear Energy in Agriculture (CENA), University of Sao Paulo (USP), using a Continuous Flow Isotopic Ratio Mass Spectrometer (CF-IRMS). Organic carbon and nitrogen are expressed as percentage of dry weight and ^{13}C and ^{15}N results are given with respect to VPDB standard and atmospheric N_2, respectively, using the conventional δ (‰) notation. Analytical precision is ± 0.1% and ±0.2‰, respectively.

The organic matter source will be environment-dependent with different $\delta^{13}C$, $\delta^{15}N$ and C/N compositions (e.g. Lamb et al., 2006), as follows: The C3 terrestrial plants shows $\delta^{13}C$ values between −32‰ and −21‰ and C/N ratio > 12, while C4 plants have $\delta^{13}C$ values ranging from −17‰ to −9‰ and C/N ratio > 20 (Deines, 1980; Meyers, 1994; Tyson, 1995). In C3-dominated environments, freshwater algae have $\delta^{13}C$ values between −25‰ and −30‰ (Meyers, 1994; Schidlowski et al., 1983) and marine algae around −24‰ to −16‰ (Haines, 1976; Meyers, 1994). In C4-dominated environments, algae can have $\delta^{13}C$ values ≤16‰ (Chivas et al., 2001). Bacteria have $\delta^{13}C$ values ranging from −12‰ to −27‰ (Coffin et al., 1989). In general, bacteria and algae have C/N ratios of 4–6 and <10, respectively (Meyers, 1994; Tyson, 1995).

Fluvial $\delta^{13}C_{POC}$ values result from freshwater phytoplankton (−25‰ to −30‰) and particulate terrestrial organic matter (−25‰ to −33‰). However, marine $\delta^{13}C_{POC}$ ranges from −23‰ to −18‰ (e.g. Barth et al., 1998; Middelburg and Nieuwenhuize, 1998). Peterson et al. (1994) found values from marine $\delta^{13}C_{DOC}$ between −22‰ and −25‰, and freshwater between −26‰ and −32‰. Thornton and McManus (1994) and Meyers (1997) used $\delta^{15}N$ values to differentiate organic matter from aquatic (>10.0‰) and terrestrial plants (~0‰).

Radiocarbon dating

Five bulk samples of ~ 2g each were used for radiocarbon dating (Table 3). The sediment samples were checked and physically cleaned under the microscope. The residual material was then extracted with 2% HCl at 60°C for 4 h, washed with distilled water until neutral pH and dried (50°C). The sediment organic matter was analyzed by Accelerator Mass Spectrometry (AMS) at the Center for Applied Isotope Studies (Athens, Georgia, USA). Radiocarbon ages are reported in years before AD 1950

Table 3. Radiocarbon dates (AMS) of the samples

Sample	Lab. number	Depth (cm)	Radiocarbon age (yr BP)	2σ calibration (cal. yr BP)	Dated material
MAC 20	UGAMS 5311	20	660 ± 25	600–560	sed. org. matter
MAC 145	UGAMS 5312	145	4470 ± 30	5290–5150	sed. org. matter
MAC 200	UGAMS 5313	200	4790 ± 30	5560–5470	sed. org. matter
AM 60	UGAMS 5314	60	1240 ± 30	1260–1080	sed. org. matter
AM 100	UGAMS 5315	100	2270 ± 25	2350–2300	sed. org. matter

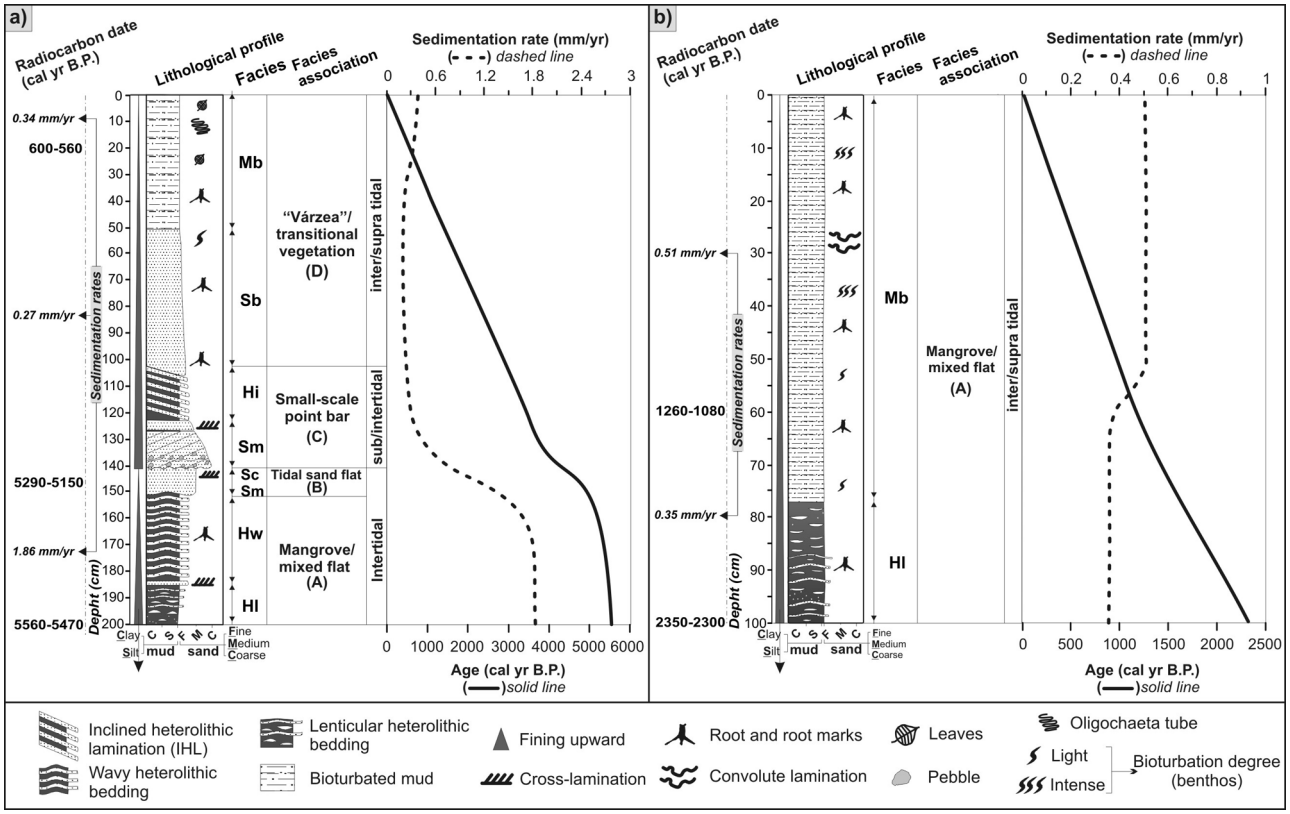

Figure 2. Graphic sedimentary log of the (a) MAC and (b) AM core

(yr BP) normalized to $\delta^{13}C$ of −25‰ VPDB and in cal. yr BP with precision of 2σ (Reimer et al., 2004).

Results and discussion

$\delta^{13}C$ values of vegetation

Within the 15 species collected, which include the most representative vegetation of the study site, the $\delta^{13}C$ values indicated a predominance of C3 plants (Table 2). The contribution of C4 to the $\delta^{13}C$ signal in sediment is restricted to the *Panicum* sp. (Poaceae) and *Paspalum repens* Berg. (Poaceae) and CAM plants to *Sesuvium* sp. (Aizoaceae) (Ramani et al., 2006).

Radiocarbon date and sedimentation rates

Radiocarbon dating of the MAC core at depths of 200 cm, 145 cm, and 20 cm produced ages of 5560–5470 cal. yr BP, 5290–5150 cal. yr BP and 600–560 cal. yr BP, respectively. Based on the ratio between the depth intervals (mm) and the mean time range, the sedimentation rates of MAC core are about 1.86 mm/yr (200–145 cm), 0.27 mm/yr (145–20 cm) and 0.34 mm/yr (20–0 cm). Two radiocarbon dates from AM core at 100 and 60 cm displayed ages of 2350–2300 cal. yr BP and 1260–1080 cal. yr BP, respectively (Table 3). The sedimentation rates are 0.35 mm/yr (100–60 cm) and 0.51 mm/yr (60–0 cm) (Figure 2).

Sediments deposited on vegetated tidal flats of Marajó Island (0.3–1 mm/yr, Behling et al., 2004), Salinopólis and the town of São Caetano (1.7–5.6 mm/yr, Cohen et al., 2009) and Bragança Peninsula (0.6–0.8 mm/yr, Cohen et al., 2005; 0.2–0.4 mm/yr, Vedel et al., 2006) on northern Brazilian coast presented similar sedimentation rates.

Facies descriptions

The sediment cores consist mostly of bioturbated mud and sand, heterolithic deposits, coarse to fine sands with cross-lamination and massive sand (Figure 2, Table 4). These lithologies are partially organized into a fining upward cycle. Pollen and spore records, $\delta^{13}C$, $\delta^{15}N$ and C/N values were added to facies characteristics in order to define four facies associations that represent typical tidal flat settings.

Facies association A (Mangrove/mixed flat). This association occurs in the lowest part of the MAC core from 5560–5470 cal. yr BP until 5290–5150 cal. yr BP, and throughout the AM core from 2350–2300 cal. yr BP until the present (Figure 2). These deposits feature mud with flat lenses of rippled sand (facies Hl and Hw) that indicate low-energy flow with mud deposition from suspension and periodic sand inflows, mostly through migration of isolated ripples (Reineck and Wunderlich, 1968). Besides these structures,

Table 4. Summary of facies descriptions and sedimentary process in the sediment cores

Facies	Description	Process
Lenticular heterolithic (Hl)	Greenish gray mud with single and connected flat lenses of pale olive, rippled fine to very fine sand.	Low-energy flows with mud deposition from suspension, but with periodic sand inflows through migration of isolated ripples.
Wavy heterolithic (Hw)	Greenish gray, wavy mud layers in alternation with pale olive, ripple-bedded fine sand layers.	Equal periods of mud and sand deposition from suspension and bedload transport, respectively.
Bioturbated mud (Mb)	Light yellowish brown and pale olive mud with many roots, root marks, dwelling structures and diffused fine sands following the root traces and benthic tubes.	Diffused mixture of sediments and alternating colors by intense bioturbation and diagenic process, respectively.
Cross-laminated sand (Sc)	Light olive gray, well sorted, fine to medium sand with current ripple cross-lamination.	Migration of small ripples during low-energy, unidirectional flows.
Massive sand (Sm)	Dark reddish brown and light yellowish brown moderately to poorly sorted, medium to coarse sand and locally angular to subangular ferruginous pebbles.	The massive nature may indicate a rapid sedimentation. In the case of the gravel class occurrence, pebbles are left behind, while sands moved as bedload under relatively high-energy flows.
Inclined heterolithic (Hi)	Parallel inclined laminae of light gray fine sand and pale olive mud with dip of ~6°.	Lateral accretion with sand and mud deposited during low-energy flows of a small-scale meandering creek.
Bioturbated sand (Sb)	Pale olive silty sand with light gray mottles, many roots, root traces in growth position and dwelling structures.	Sediment homogenization and mottling by biological activity and diagenic process, respectively.

the AM core presents mud with convolute lamination, many bioturbation features (facies Mb) such as roots, root marks and dwelling structures produced by the benthic fauna. Probably, convolute lamination was produced by localized differential forces acting on a hydroplastic sediment layer, commonly found on mud flats (Collinson et al., 2006).

The pollen assemblages of association A correspond to Zone MAC 1 (Figure 3), AM1 and AM2 (Figure 4). Zone MAC 1 was subdivided in Subzone MAC 1a and MAC 1b. Subzone MAC 1a (5560–5470 cal. yr BP to ~ 5430 cal. yr BP) is characterized by the predominance of mangrove pollen, mainly constituted by *Rhizophora* (20–75%). 'várzea' pollen of Araliaceae, Arecaceae, *Ilex*, *Mauritia* and Mimosoideae appear with very low percentages (<10%). Even profilic producers of windblown pollen such as Poaceae (Colinvaux et al., 1999) show low values (18–40%). However, Poaceae pollen (40–73%) increases in the Subzone MAC 1b (~5430 to 5290–5150 cal. yr BP). *Rhizophora* pollen (0–24%) becomes less frequent. Arecaceae (0–22%), Euphorbiaceae and *Mauritia* (~10%) are the main representatives of 'várzea' pollen.

Zone AM 1 (2350–2300 cal. yr BP to 1260–1080 cal. yr BP) reveals a heterogeneous vegetation assemblage (Figure 4). Inundated field pollen of Poaceae (18–48%), and mangrove pollen of *Rhizophora* (21–36%) and *Avicennia* (3–15%) are prevalent. *Acrostichum* (0–50%) fern is another mangrove indicator (Ng et al., 2002), but presented relatively low values. 'várzea' pollen of Euphorbiaceae (0–22%), *Pseudobombax* (0–10%) and Papilionoideae (2–5%) also showed low values. Subsequently, 'várzea' pollen progressively becomes less abundant. Inundated field pollen represented by Poaceae (20–40%), Amaranthaceae (3–10%) and Malpighiaceae (0–10%), jointly with mangrove pollen of *Rhizophora* (13–49%) and *Avicennia* (2–22%) exhibited high values, but mangrove pollen decreases towards the end of zone AM 1. Nevertheless, in zone AM 2 (1260–1080 cal. yr BP to modern), mangrove pollen is very well represented by *Rhizophora* (20–60%) and *Avicennia* (18–40%). *Acrostichum* (23–98%) fern reached its highest values in this zone.

The sediment $\delta^{13}C$ values ranging between −25‰ and −27.6‰ indicate the dominance of C3 plants (−32‰ to −21‰; Deines, 1980) and/or a mixture of freshwater algae (−26‰ to −30‰, Meyers, 1994; Schidlowski et al., 1983) and perhaps marine DOC (−22‰ to −25‰; Peterson et al., 1994). The $\delta^{15}N$ in the range of 2.1–7.5‰ suggests a mixture of terrestrial plants (~0‰) and aquatic organic matter (>10‰, Meyers, 1997; Thornton and McManus, 1994). The C/N values (11–20) also indicate a mixture of organic matter from vascular plants and algae (< 10 algae dominance and > 12 vascular plants; Meyers, 1994; Tyson, 1995), and the binary diagram between the $\delta^{13}C$ and C/N reveals contribution of marine and freshwater Dissolved Organic Carbon (DOC; Figures 5, 6 and 7).

Facies association B (Tidal sand flat). The association B begins around 5290–5150 cal. yr BP in the MAC core (Figure 2). It consists of massive sands (facies Sm) and cross-laminated sand (facies Sc), which record relatively low and high flow energy with current action shaping the bedform, inducing the migration of small sand ripples (Reineck and Singh, 1980). Pollen was not found in the association B, which corresponds to Subzone MAC 2a1 (Figure 3).

The sediment $\delta^{13}C$ values ranging between −25.8‰ and −26.3‰ suggest the contribution of C3 plants and fluvial Particulate Organic Carbon (POC; −25‰ to −30‰; Barth et al., 1998). The $\delta^{15}N$ values (4.3‰ to 5.4‰) indicate higher aquatic influence than in association A. Furthermore, the C/N values exhibit a reduction to 5.5 and 6.6 (Figure 5), reinforcing the contribution of aquatic materials because of fluvial influence through the relative contribution of phytoplankton (5 to 7; Meyers, 1994; Tyson, 1995). The relationship between $\delta^{13}C$ and C/N indicates freshwater algae as the main source of the organic matter accumulated in this facies association (Figure 7).

Facies association C (Small-scale point-bar). This association only occurs in the MAC core (Figure 2). Given calibrated ages below and above association C (5290–5150 cal. yr BP and ~ 3700 cal. yr BP), a sedimentary gap of 1000 years probably occurred because of the migration of a meandering creek. The association presents erosive base, medium to coarser sands with scattered ferruginous pebbles (facies Sm), which is overlaid by inclined sand and mud (facies Hi). Association C is a product of point-bar lateral accretion within a small-scale meandering creek draining intertidal mudflats, where periodic fluctuations of current

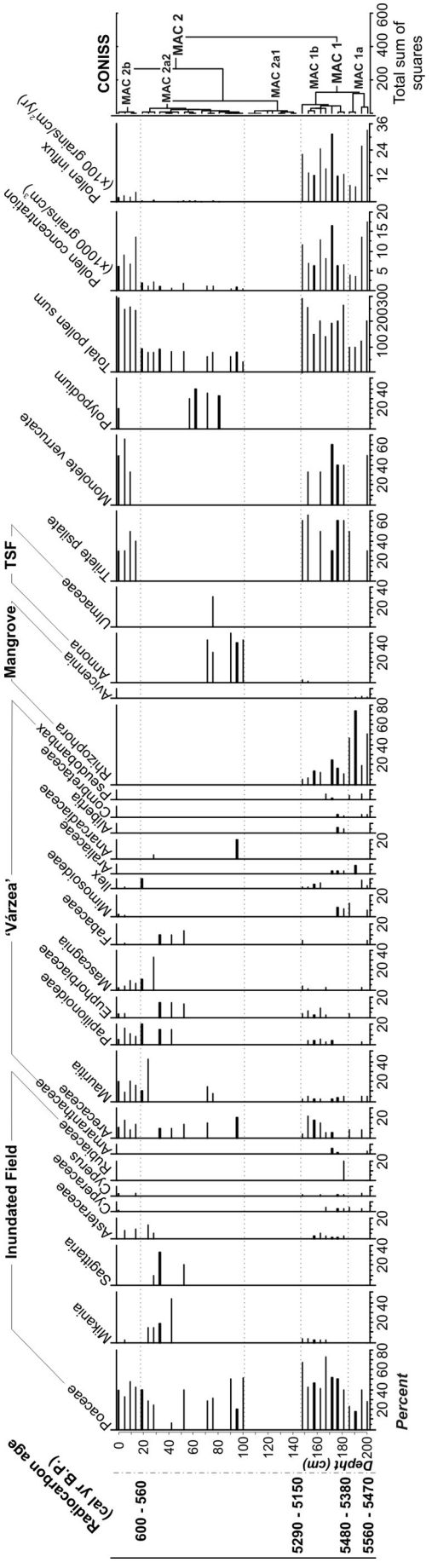

Figure 3. Pollen diagram of the MAC core

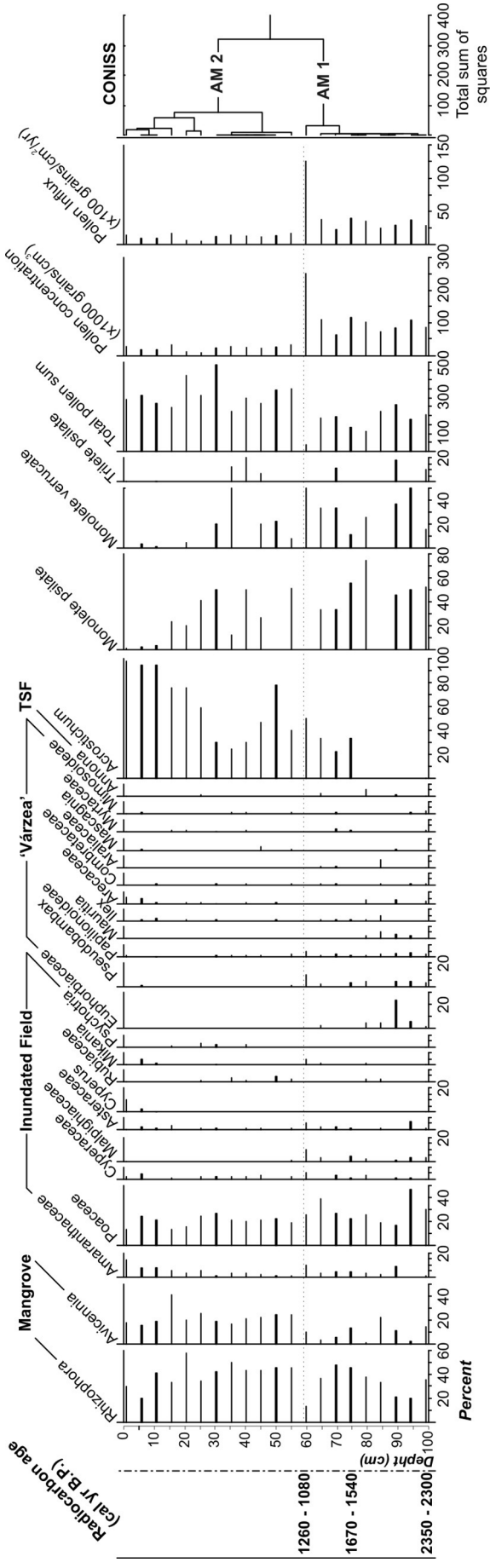

Figure 4. Pollen diagram of the AM core

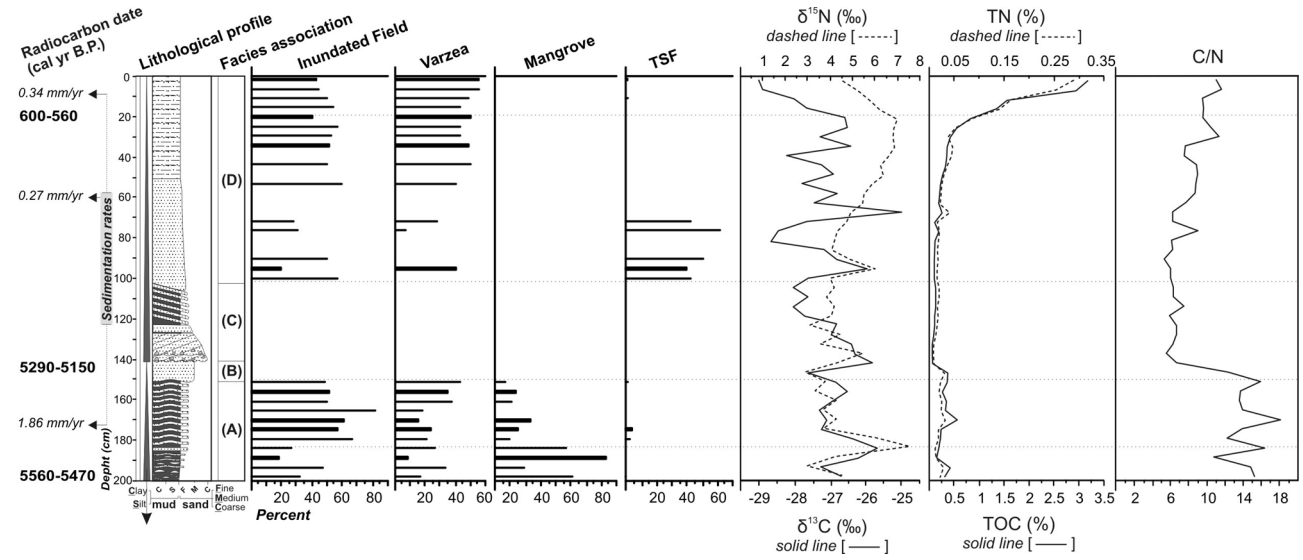

Figure 5. Interproxy records of the MAC core

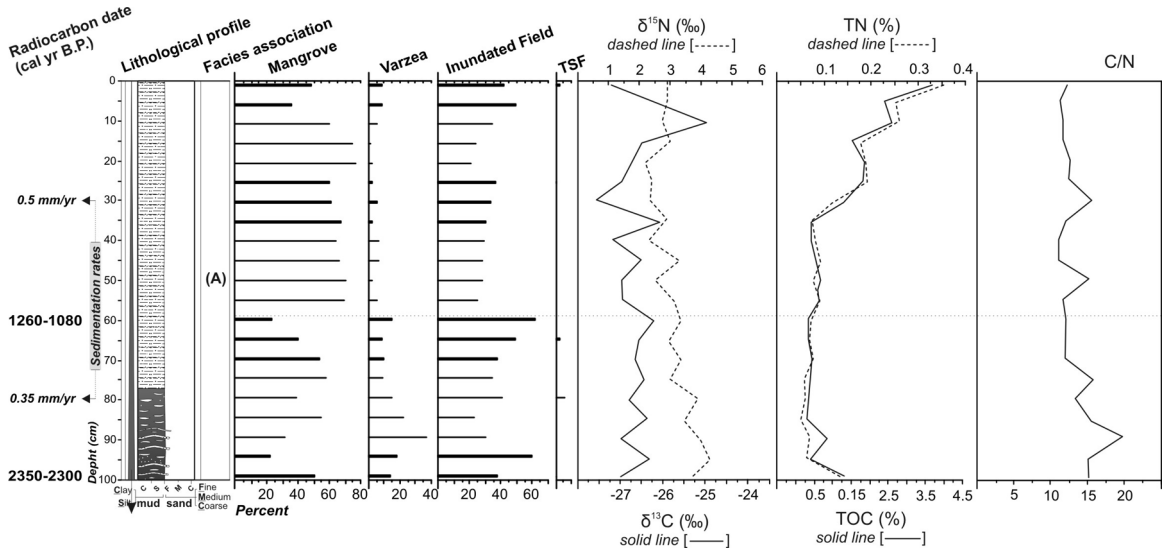

Figure 6. Interproxy records of the AM core

velocity/direction and water levels inherent to the tidal cycles, allowed sand and mud deposition during periods of high (ebb or flood tidal current) and low (slack water) energy flows, respectively (Thomas et al., 1987). The association C also integrates Subzone MAC 2a1 (Figure 3).

Sediment $\delta^{13}C$ values (−26.4‰ to −28‰) were more depleted in ^{13}C than association B, which is indicative of a greater contribution of fluvial POC. The $\delta^{15}N$ values (3‰ to 4.4‰), suggest a mixture of aquatic and terrestrial organic matter. However, the C/N values (5.8 to 6.6) indicate higher contribution of aquatic organic matter (Figure 5), as well as the relationship between $\delta^{13}C$ and C/N also indicates higher contribution of freshwater algae (Figure 7).

Facies association D ('Várzea'/transitional vegetation). The association D only occurs in the MAC core. It presents silty sand (facies Sb) and mud (facies Mb) with many roots, root marks of species with diffuse/fasciculated root systems, fragments of leaves, Oligochaeta tubes and mottling features (Figure 2), which may indicate diagenetic process in a vegetated substrate (e.g. Retallack, 2001).

This association corresponds to Subzone MAC 2a2 and MAC 2b (Figure 3). The Subzone MAC 2a2 (~3700 to 600–560 cal. yr BP) presents TSF and inundated field pollen of *Annona* and Poaceae (0–50%). Inundated field pollen of *Mikania* (0–44%), Poaceae (0–40%), *Sagittaria* (0–35%) and 'várzea' pollen of Euphorbiaceae (0–15%), *Mauritia* (0–43%), *Mascagnia* (0–33%), Papilionoideae (0–20%) increase toward the top. *Polypodium* (0–40%) is the only fern found in MAC 2a2. In the Zone MAC 2b (600–560 cal. yr BP to modern), Arecaceae (10–18%), *Mauritia* (10–20%), Papilionoideae (6–16%), *Mascagnia* (3–10%) and Poaceae (32–47%) pollen are well correlated to the modern vegetation at the sampling site. The incipient pollen results in the Subzone MAC 2a2 of inundated field (0–62%), TSF (0–60%) and 'várzea' (0–50%) suggest that inundated field and other successional vegetation act as pioneers for the stabilization of a new organic horizon for TSF development, until the expansion of 'várzea' forests at 600–560 cal. yr BP.

The sediment $\delta^{13}C$ values varied from −25.9‰ to −29‰, the $\delta^{15}N$ from 3.6‰ to 6.9‰ and the C/N values from 5.2 to 11.6. These are indicative of a mixture of terrestrial and aquatic organic matter (Figure 5). The binary diagram of $\delta^{13}C$ and C/N

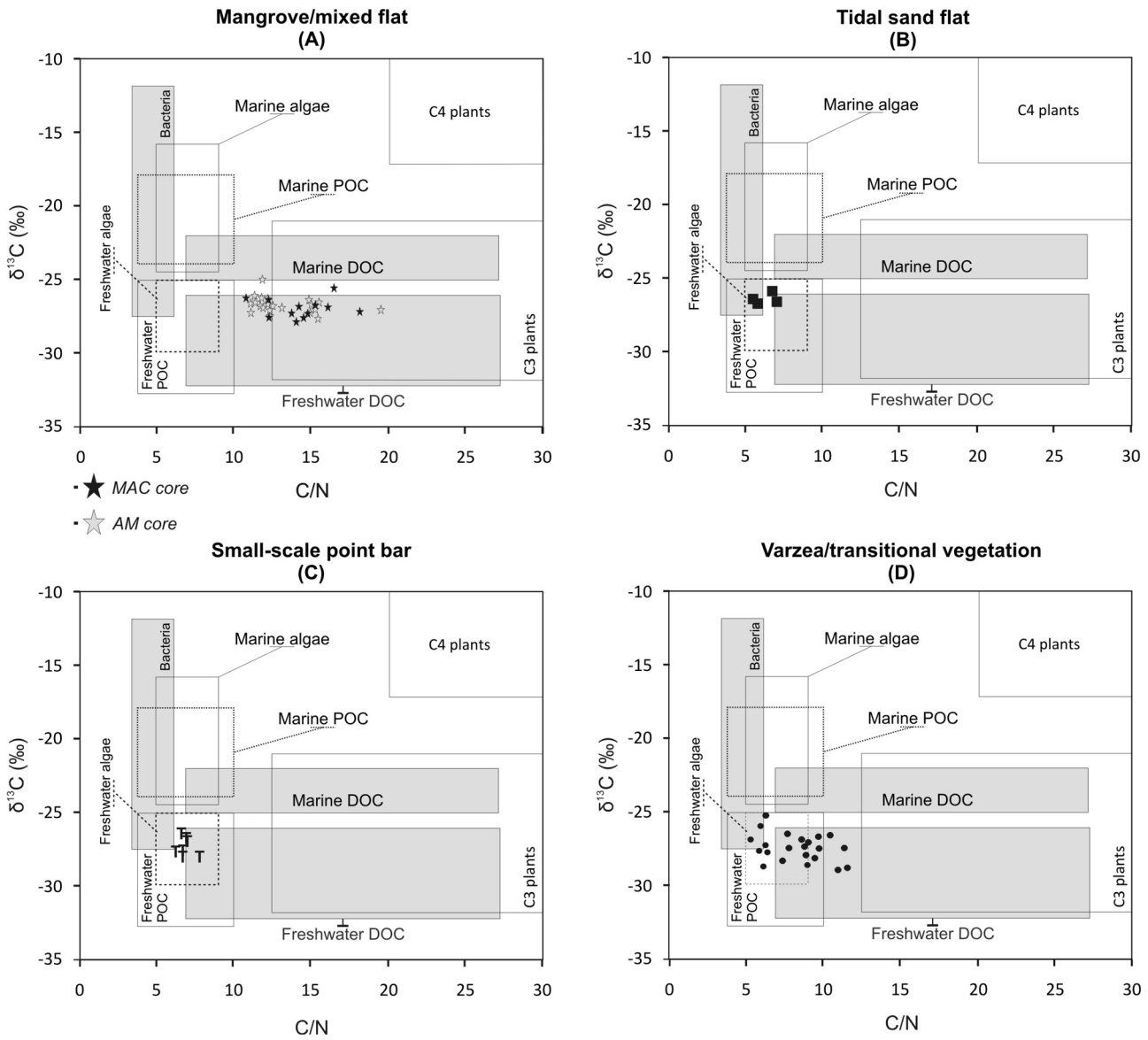

Figure 7. Binary diagram of $\delta^{13}C$ and C/N for each sedimentary facies in the study area with interpretation of carbon sources based on typical ranges recorded in several coastal environments (Deines, 1980; Haines, 1976; Lamb et al., 2006; Meyers, 1994; Middelburg and Nieuwenhuize, 1998; Peterson et al., 1994; Raymond and Bauer, 2001; Schidlowski et al., 1983; Tyson, 1995 and references therein)

values reinforces the influence of freshwater DOC and POC (Figure 7).

Palaeoenviromental interpretation

The data suggest mangrove predominance and the accumulation of brackish water organic matter over a tidal mud flat from Macapá littoral around 5560–5470 cal. yr BP (Figure 5). Between 5560–5470 and 5290–5150 cal. yr BP, the data suggests retraction of mangrove and expansion of Arecaceae and herbaceous vegetation followed by an increase in the contribution of freshwater organic matter (Figure 8). Near the study site (~ 8 km), palaeoecological records from Lake Márcio and Tapera revealed the occurrence of mangrove forests between 8060 and 5840 cal. yr BP, and the replacement of mangrove by freshwater vegetation until 5300 cal. yr BP (Toledo and Bush, 2007).

The point bar sequence found in the Macapá site reveals a common reworking process of the tidal flat through the lateral migration of a meandering creek (e.g. Reineck, 1958; Thomas et al., 1987), with later development of transitional vegetation under freshwater influence. Following the natural vegetation succession under relatively stable climate and hydrological conditions, the expansion of 'várzea' forests occurred since 600–560 cal. yr BP until the present (Figure 8).

Regarding the littoral of the town of Amapá (150 km away from the mouth of the Amazon River, Figure 1), the mangrove forests have colonized tidal mud flats during the last 2350–2300 cal. yr BP. However, the *Acrostichum* sp. (mangrove ferns) has expanded over the last ~1500 cal. yr BP. This fern tends to invade open areas under relatively less salty water and high rainfall conditions (Medina et al., 1990). Furthermore, the current distribution of freshwater vegetation near the town of Amapá (Figure 1) suggests a continuous colonization of 'várzea' vegetation to the detriment of mangrove during the late Holocene.

Despite this fact that this work is restricted to data on depositional environment, palaeovegetation changes and organic matter sources, we consider it appropriate to propose a hypothesis to explain this environmental alteration through palaeoclimate changes affecting the Amazon River inflow during the Holocene. Thus, after the postglacial sea-level rise, the relative sea level along the Northern Brazilian littoral reached the current sea level

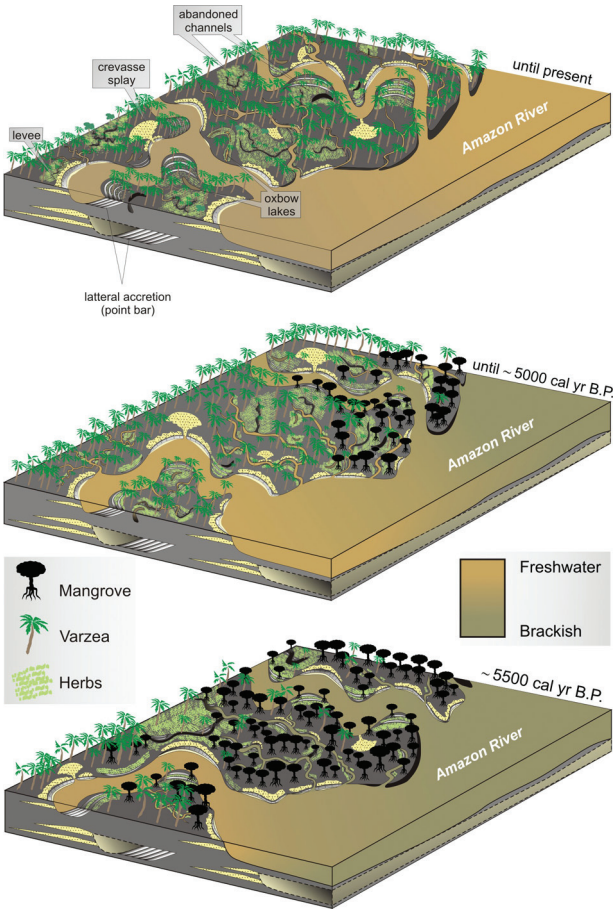

Figure 8. Schematic representation of successive phases of sediment accumulation and vegetation change in the study area according to Amazon River inflow in a stationary littoral

between 7000 and 5000 yr BP, and did not show significant oscillations during the last 5000 years (Cohen et al., 2005; Souza Filho et al., 2006). However, our data show that after the sea-level rise an increase in fluvial influence occurred along the study site. Today, the Amazon River discharge has a great influence on the salinity gradient along the tidal flats, limiting the mangrove vegetation to the northwestern Amapá littoral closer to the Atlantic Ocean (Guimarães et al., 2010).

The northern Brazilian mangroves are part of a wetland system that extends for almost 480 km and holds one of the world's largest mangrove areas (Kjerfve and Lacerda, 1993). The continuity of this mangrove littoral is interrupted by the zone influenced by discharge of the Amazon River, where the 'várzea' vegetation dominates (Cohen et al., 2008). The mangrove zones are the response to the gradients of tidal inundation frequency, waterlogging, nutrient availability and sediment salt concentrations across the intertidal area (Hutchings and Saenger, 1987; Wolanski et al., 1990). The geomorphic setting of mangrove systems also comprises a range of inter-related factors such as substrate types, coastal processes, sediment delivery, and freshwater delivery, all of which influence the occurrence and survivorship of mangroves (Semeniuk, 1994). However, an empirical model based on an ecohydrological approach, which allowed the integration of hydrographical, topographical and physicochemical information with vegetation characteristics of mangroves and marshes, indicates that under the same morphological condition, change in pore water salinity is the main factor displacing the wetlands boundaries on northern Brazil (Cohen and Lara, 2003; Lara and Cohen, 2006). The relations between mangrove and sediment geochemistry have been widely investigated (Alongi et al., 2000; Baltzer, 1970; Clark et al., 1998; Hesse, 1961; Lacerda et al., 1995; Snedaker, 1978; Walsh, 1974; Youssef and Saenger, 1999). The Pará Littoral-Northern Brazil (Behling et al., 2001; Cohen et al., 2005), follows well-known patterns, where salinity excludes certain species (Snedaker, 1978), leading to characteristic patterns of species zonation and predictable types of community structure (Menezes et al., 2003), where the mangroves are more tolerant to sediment salinity than 'várzea' forest (Gonçalves-Alvim et al., 2001).

Regarding the river dynamics affecting the local vegetation and geochemical proxies, only the 105–140 cm interval of the core MAC presented a sedimentary structure that indicates migration of a meandering creek. This interval is a product of point-bar lateral accretion within a small-scale meandering creek (Thomas et al., 1987). Likely, following this dynamic, the organic matter and sediments are products of the reworking of material from the margin along the channel. Indeed, this mechanism may disturb a continuous sequence of pollen and isotopic records. However, as described in the Facies Association C of this work, this process may be identified by the sedimentary facies associated to the pollen and isotopic data (e.g. Miranda et al., 2009). Other sedimentary facies of the studied cores indicate stable tidal sand/mud flats colonized by mangrove and/or 'várzea' vegetation. Thus, this depositional environment accumulated sediment with pollen and organic matter that reflects the main vegetation and organisms colonizing the study site during that time.

Therefore our hypothesis is that, during the mid Holocene, the Amazon River inflow was lower than today, which allowed an increase of marine influence in sector 2 (Figure 1d). Afterward, the retraction of mangrove and expansion of freshwater vegetation during the late Holocene indicates the return of more humid climate conditions and rise of Amazon River inflow.

Along the littoral of the town of Amapá, at least during the last 2350–2300 cal. yr BP, the marine influence allowed the maintenance of mangrove vegetation and the increase in Amazon River inflow during the late Holocene was not strong enough to result in the total replacement of mangrove by 'várzea' and/or inundated field, such as occurred on the Macapá site after 5290–5150 cal. yr BP.

Several palaeoecological studies in the Amazon region also indicate drier climate during the mid Holocene, and a wet period during the late Holocene (e.g. Absy et al., 1991; Behling and Hooghiemstra, 2000; Bush and Colinvaux, 1988; Bush et al., 2007; Desjardins et al., 1996; Gouveia et al., 1997; Pessenda et al., 1998, 2001; Sifeddine et al., 1994, 2001; Weng et al., 2002).

Conclusion

The tidal flat data analyzed indicate significant vegetation changes. The marine influence and resultant mangrove expansion occurred between 5560–5470 cal. yr BP and ~5430 cal. yr BP. Between ~5430 and 5290–5150 cal. yr BP, the mangrove retreated and freshwater vegetation expanded, which suggests a decrease in marine influence. During the late Holocene, freshwater vegetation developed along the tidal flat from Macapá site. However, on the northwestern Amapá littoral, which lies 150 km away from the mouth of Amazon River, the mangrove forests have colonized part of the tidal mud flats during the last 2350–2300 cal. yr BP. This suggests that marine influence allowed the maintenance of this vegetation, and the increase in fluvial inflow did not result in a complete replacement of mangrove by freshwater vegetation.

Acknowledgements

The authors thank the members of the Laboratório de Dinâmica Costeira – Universidade Federal do Pará and the Laboratório de Carbono 14 – Centro de Energia Nuclear na Agricultura, Universidade de São Paulo-USP.

Funding

This work was funded by CNPq (Project 562398/2008-2). The first and second authors hold a scholarship from CNPq (Process 143518/2008-9 and 302943/2008-0).

References

Absy ML, Clief A, Fournier M, Martin L, Servant M, Siffeddine A et al. (1991) Mise en évidence de Quatre phases d'ouverture de la forêt dense dans le sud-estde L'Amazonie au cours des 60,000 dernières années. Première comparaison avec d'autres régions tropicales. *Comptes Rendus Academie des Sciences Paris* 312: 673–678.

Allison MA, Lee MT, Ogston AS and Aller RC (2000) Origin of Amazon mudbanks along the northeastern coast of South America. *Marine Geology* 163: 241–256.

Alongi DM, Tirendi F and Clough BF (2000) Below-ground decomposition of organic matter in forests of the mangrove *Rhizophora stylosa* and *Avicennia marina* along the arid coast of Western Australia. *Aquatic Botany* 68: 97–122.

ANA (2003) *Hydrological Information System*. Brazilian National Water Agency. Online data set, 14.3 MB, http://hidroweb.ana.gov.br/baixar/mapa/Bacia1.zip

Baltzer F (1970) *Etude sédimentologique du marais de Mara (Côte ouest de la Nouvelle Calédonie) et de formations quaternaires voisines*. Mémoires expédition française sur les récifs coralliens de la Nouvelle Calédonie, Foundation Singer-Polignac 4, 146–169.

Barth JAC, Veizer J and Mayer B (1998) Origin of particulate organic carbon in the upper St. Lawrence: Isotopic constraints. *Earth and Planetary Science Letters* 162: 111–121.

Beardsley RC, Candela J, Limeburner R, Geyer WR, Lentz SJ, Castro BM et al. (1995) The M2 tide on the Amazon shelf. *Journal of Geophysical Research* 100: 2283–2319.

Behling H and Costa ML (2000) Holocene environmental changes from the Rio Curuá record in the Caxiuanã region, eastern Amazon Basin. *Quaternary Research* 53: 369–377.

Behling H and Costa ML (2001) Holocene vegetation and coastal environmental changes from Lago Crispim in northeastern Pará State, northern Brazil. *Palaeogeography*, *Palaeoclimatology*, *Palaeoecology* 114: 145–155.

Behling H and Hooghiemstra H (2000) Holocene Amazon rain forest – Savanna dynamics and climatic implications: High resolution pollen record Laguna Loma Linda in eastern Colombia. *Journal of Quaternary Science* 15: 687–695.

Behling H, Cohen MCL and Lara RJ (2001) Studies on Holocene mangroves ecosystem of the Bragança Peninsula in north-eastern Pará, Brazil. *Palaeogeography*, *Palaeoclimatology*, *Palaeoecology* 167: 225–242.

Behling H, Cohen MCL and Lara RJ (2004) Late Holocene mangrove dynamics of Marajó Island in Amazonia, northern Brazil. *Vegetation History and Archaeobotany* 13: 73–80.

Bezerra PEL, Oliveira W, Regis WDE, Brazão JEM, Gavinho J and Coutinho RCP (1990) Amazônia legal: Zoneamento das potencialidades e dos recursos naturais. In: Instituto Brasileiro de Geografia e Estatística, Superintendência de Desenvolvimento da Amazônia. *Projeto zoneamento das potencialidades dos recursos naturais da Amazônia: geologia, solos e vegetação*. Div. 5. Rio de Janeiro, 9–89.

Bush MB and Colinvaux PA (1988) A 7000yr vegetational history from lowland Amazon, Ecuador. *Plant Ecology* 76: 141–154.

Bush MB, Silman MR and Listopad CMCS (2007) A regional study of Holocene climate change and human occupation in Peruvian Amazonia. *Journal of Biogeography* 34: 1342–1356.

Carvalho FP, Costa Neto SV, Costa WJP, Coutinho RS, Figueira ZR, Figueiredo SL et al. (2006) *Atlas Zoneamento Costeiro Estuarino do Estado do Amapá*. Macapá, PNMA/SQA/MMA, 77 pp.

Chivas AR, Garcia A, Van der Kaars S, Couapel MJJ, Holt S, Reeves JM et al. (2001) Sea-level and environmental changes since the last interglacial in the Gulf of Carpentaria, Australia: An overview. *Quaternary International* 83–85: 19–46.

Clark MW, McConchie DM, Lewis DW and Saenger P (1998) Redox stratification and heavy metal partitioning in Avicennia-dominated mangrove sediments: A geochemical model. *Chemistry Geology* 149: 147–171.

Coffin RB, Fry B, Peterson BJ, Wright RT (1989) Carbon isotopic compositions of estuarine bacteria. *Limnology and Oceanography* 34: 1305–1310.

Cohen MCL and Lara RJ (2003) Temporal changes of vegetation boundaries in Amazonia: Application of GIS and Remote sensing techniques. *Wetlands Ecology and Management* 11: 223–231.

Cohen MCL, Souza Filho PWM, Lara RJ, Behling H and Angulo RJ (2005) A model of Holocene mangrove development and relative sea-level changes on the Bragança Peninsula (Northern Brazil). *Wetlands Ecology and Management* 13: 433–443.

Cohen MCL, Lara RJ, Smith CB, Angélica RS, Dias BS and Pequeno T (2008) Wetland dynamics of Marajó Island, northern Brazil, during the last 1000 years. *Catena* 76: 70–77.

Cohen MCL, Lara RJ, Smith CB, Matos HRS and Vedel V (2009).Impact of sea-level and climatic changes on the Amazon coastal wetlands during the late Holocene. *Vegetation History and Archaeobotany* 18: 425–439.

Colinvaux PA, De Oliveira PE and Patiño JEM (1999) *Amazon Pollen Manual and Atlas - Manual e Atlas Palinológico da Amazônia*. Amsterdam: Hardwood Academic, 332 pp.

Collinson J, Mountney N and Thompson D (2006) *Sedimentary Structures*. (Third edition) Terra Publishing, 292 pp.

Costa JB, Hasui Y, Bemerguy RL, Soares-Júnior AV and Villegas J (2002) Tectonics and paleogeography of the Marajó Basin, northern Brazil. *Anais da Academia Brasileira de Ciências* 74: 519–531.

Costa Neto SV (2004) *Relatório de vegetação: Subsídio ao diagnostico sócio ambiental*. Relatório Técnico. Macapá, IEPA/GERCO, 32 pp.

Costa Neto SV and Silva MS (2004) *Vegetação do setor costeiro estuarino do estado do Amapá*. Instituto de Pesquisas Científicas e Tecnológicas do Estado do Amapá. Governo do Estado do Amapá. Cap. 5. Projeto Zoneamento Econômico-Ecológico do setor costeiro estuarino: Diagnóstico sócio ambiental participativo do setor costeiro estuarino, 72–96.

Costa Neto SV, Senna C, Tostes LCL and Silva SRM (2007) Macrófitas aquáticas das Regiões dos Lagos do Amapá, Brasil. *Revista Brasileira de Biociências* 5: 618–620.

CPRM (2010) *Geological Information System*. Brazilian Geological Service. Online data set, Folhas NA/SA-22 23 MB, http://geobank.sa.cprm.gov.br/

Dalrymple RW and Choi K (2007) Morphologic and facies trends through the fluvial-marine transition in tide-dominated systems: A schematic framework for environmental and sequence-stratigraphic interpretation. *Earth-Science Reviews* 81: 135–174.

Deines P (1980) The isotopic composition of reduced organic carbon. In: Fritz P and Fontes JC (eds) *Handbook of Environmental Isotope Geochemistry*. *The Terrestrial Environment, Vol.1*. Amsterdam: Elsevier, 329–406.

Desjardins T, Filho AC, Mariotti A, Chauvel A and Girardin C (1996) Changes of the forest–savanna boundary in Brazilian Amazonia during the Holocene as revealed by soil organic carbon isotope ratios. *Oecologia* 108: 749–756.

Engelhart SE, Horton BP, Roberts DH, Bryant CL and Corbett DR (2007) Mangrove pollen of Indonesia and its suitability as a sea-level indicator. *Marine Geology* 242: 65–68.

Faegri K and Iversen J (1989) *Textbook of Pollen Analyses*. Chichester: John Wiley and Sons LTD, 328 pp.

Freycon V, Krencker M, Schwartz D, Nasi R and Bonal D (2009) The impact of climate changes during the Holocene on vegetation in northern French Guiana. *Quaternary Research* 73: 220–225.

Gallo MN and Vinzon S (2005) Generation of over tides and compound tides in Amazon estuary. *Ocean Dynamics* 55: 441–448.

Gonçalves-Alvim SJ, Vaz dos Santos MCF and Fernandes GW (2001) Leaf gall abundance on *Avicennia germinans* (Avicenniaceae) along an interstitial salinity gradient. *Biotropica* 33: 69–77.

Gouveia SEM, Pessenda LCR, Aravena R, Boulet R, Roveratti R and Gomes BM (1997) Dinâmica de vegetações durante o Quaternário recente no sul do Amazonas indicada pelos isótopos do carbono (^{12}C, ^{13}C e ^{14}C). *Geochimica Brasiliensis* 11: 355–367.

Grimm EC (1987) CONISS: A FORTRAN 77 program for stratigraphically constrained cluster analysis by the method of the incremental sum of square. *Computer and Geosciences* 13: 13–35.

Guimarães JTF, Cohen MCL, França MC, Lara RJ and Behling H (2010) Model of wetland development of the Amapá coast during the late Holocene. *Anais da Academia Brasileira de Ciências* 82: 451–465.

Haines EB (1976) Stable carbon isotope ratios in biota, soils and tidal water of a Georgia salt marsh. *Estuarine and Coastal Marine Science* 4: 609–616.

Hesse M, Halbritter H, Zetter R, Weber M, Buchner R, Frosch-Radivo A et al. (2008) *Pollen Terminology*: *An Illustrated Handbook*. New York: Springer, 264 pp.

Hesse PR (1961) Some differences between the soils of *Rhizophora* and *Avicennia* mangrove swamp in Sierra Leone. *Plant Soil* 14: 335–346.

Horton BP, Gibbard PL, Milne GM, Morley RJ, Purintavaragul C and Stargardt JM (2005) Holocene sea levels and palaeoenvironments of the Malay-Thai Peninsula, southeast Asia. *The Holocene* 15: 1199–1213.

Hutchings P and Saenger P (1987) *Ecology of Mangroves*. Queensland University Press, 388 pp.

Kjerfve B and Lacerda LD (1993) Mangroves of Brazil. In: Lacerda LD (ed.) *Conservation and Sustainable Utilization of Mangrove Forests in Latin*

America and Africa Regions. *Part I – Latin America*. Okinawa: ITTO/ International Society for Mangrove Ecosystems, 245–272.

Klein GV (1971) A sedimentary model for determining paleotidal range. *Geological Society of America Bulletin* 82: 2585–2592.

Lacerda LD, Ittekkot V, Patchineelam SR (1995) Biogeochemistry of mangrove soil organic matter: A comparison between *Rhizophora*, *Avicennia* soils in south-eastern Brazil. *Estuarine, Coastal and Shelf Science* 40: 713–720.

Lamb AL, Wilson GP and Leng MJ (2006) A review of coastal palaeoclimate and relative sea-level reconstructions using $\delta^{13}C$ and C/N ratios in organic material. *Earth-Science Reviews* 75: 29–57.

Lara JR and Cohen MCL (2006) Sediment porewater salinity, inundation frequency and mangrove vegetation height in Bragança, North Brazil: An ecohydrology-based empirical model. *Wetlands Ecology and Management* 14: 349–358.

Latrubesse EM and Franzinelli E (2002) The Holocene alluvial plain of the middle Amazon River, Brazil. *Geomorphology* 44: 241–257.

Ledru MP (2001) Late Holocene rainforest disturbance in French Guiana. *Review of Palaeobotany and Palynology* 115: 161–176.

Lentz SJ (1995) The Amazon River plume during AMASSEDS: Subtidal current variability and the importance of wind forcing. *Journal of Geophysical Research* 100: 2377–2390.

Lentz SJ and Limeburner R (1995) The Amazon River Plume during AMASSEDS: Spatial characteristics and salinity variability. *Journal of Geophysical Research* 100: 2355–2375.

Lima MIC, Bezerra PE and Araújo HJT (1991) Sistematização da Geologia do Estado do Amapá. In: *Simpósio de geologia da Amazônia*, *vol. 3*. Belém, Anais, SBG, 322–335.

Maslin MA and Burns SJ (2000) Reconstruction of the Amazon Basin effective moisture availability over the past 14,000 years. *Science* 290: 2285–2287.

Medina E, Cuevas E, Popp M and Lugo A (1990) Soil salinity, sun exposure, and growth of *Acrostichum aureum*, the mangrove fern. *Botanical Gazette* 151: 41–49.

Menezes M, Berger U and Worbes M (2003) Annual growth rings and long-term growth patterns of mangrove trees from the Bragança peninsula, North Brazil. *Wetlands Ecology and Management* 11: 233–242.

Meyers PA (1994) Preservation of elemental and isotopic source identification of sedimentary organic matter. *Chemical Geology* 114: 289–302.

Meyers PA (1997) Organic geochemical proxies of paleoceanographic, paleolimnologic and paleoclimatic processes. *Organic Geochemistry* 27: 213–250.

Miall AD (1978) Facies types and vertical profile models in braided river deposits: A summary. In: Miall AD (ed.) *Fluvial Sedimentology*. Calgary: Canadian Society of Petroleum Geologists, 597–604.

Middelburg JJ and Nieuwenhuize J (1998) Carbon and nitrogen stable isotopes in suspended matter and sediments from the Schelde Estuary. *Marine Chemistry* 60: 217–225.

Miranda MCC, Rossetti DF and Pessenda LCR (2009) Quaternary paleoenvironments and relative sea-level changes in Marajó Island (Northern Brazil): Facies, $\delta^{13}C$, $\delta^{>15}N$ and C/N. *Palaeogeography, Palaeoclimatology, Palaeoecology* 282: 19–31.

Ng PKL, Sivasothi N, Morgany T and Murphy DH (2002) *A Guide to the Mangroves of Singapore 1*: *The Ecosystem & Plant Diversity*. Singapore Science Centre, Rev. Edition, 160 pp.

Pessenda LCR, Boulet R, Aravena R, Rosolen V, Gouveia SEM, Ribeiro AS et al. (2001) Origin and dynamics of soil organic matterand vegetation changes during the Holocene in a forest–savanna transition zone, Brazilian Amazon region. *The Holocene* 11: 250–254.

Pessenda LCR, Gouveia SEM, Aravena R, Gomes BM, Boulet R and Ribeiro AS (1998) ^{14}C dating and stable carbon isotopes of soil organic matter in forest–savanna boundary areas in southern Brazilian Amazon region. *Radiocarbon* 40: 1013–1022.

Peterson BJ, Fry B, Hullar M, Saupe S and Wright R (1994) The distribution and stable carbon isotope composition of dissolved organic carbon in estuaries. *Estuaries* 17: 111–121.

Pugh DT (1987) *Tides, Surges and Mean Sea-level*: *A Handbook for Engineers and Scientists*. London: Wiley, 486 pp.

Ramani B, Reeckb T, Debezc A, Stelzerd R, Huchzermeyera B, Schmidta A et al. (2006) *Aster tripolium* L. and *Sesuvium portulacastrum* L.: Two halophytes, two strategies to survive in saline habitats. *Plant Physiology and Biochemistry* 44: 395–408.

Raymond PA and Bauer JE (2001) Use of ^{14}C and ^{13}C natural abundances for evaluating riverine, estuarine, and coastal DOC and POC sources and cycling: A review and synthesis. *Organic Geochemistry* 32: 469–485.

Reimer PJ, Baillie MGL, Bard E, Bayliss A, Beck JW, Bertrand CJH et al. (2004) IntCal04 terrestrial radiocarbon age calibration, 26–0 ka BP. *Radiocarbon* 46: 1029–1058.

Reineck HE (1958) Longitudinale schrägschicht in Watt. *Geologische Rundschau* 47: 73–82.

Reineck HE and Singh IB (1980) *Depositional Sedimentary Environments with Reference to Terrigenous Clastics* (Second edition). Berlin: Springer-Verlag, 542 pp.

Reineck HE and Wunderlich F (1968) Classification and origin of flaser and lenticular bedding. *Sedimentology* 11: 99–104.

Retallack GJ (2001) *Soils of the Past – An Introduction to Paleopedology* (Second edition). Wiley-Blackwell, 512 pp.

Rosario RP, Bezerra MOM and Vinzon SB (2009) Dynamics of the saline front in the Northern Channel of the Amazon River – Influence of fluvial flow and tidal range (Brazil). *Journal of Coastal Research* 2: 503–514.

Roubik DW and Moreno JE (1991) *Pollen and Spores of Barro Colorado Island*. Missouri Botanical Garden, 268 pp.

Schidlowski M, Hayes JM and Kaplan IR (1983) Isotopic inferences of ancient biochemistries: Carbon, sulphur, hydrogen and nitrogen. In: Scholf JW (ed.) *Earth's Earliest Biosphere, Its Origin and Evolution*. Princeton: Princeton University Press, 149–186.

Semeniuk V (1994) Predicting the effect of sea-level rise on mangroves in northwestern Australia. *Journal of Coastal Research* 10: 1050–1076.

Sifeddine A, Fröhlich F, Fournier M, Martin L, Servant M, Soubiés F et al. (1994) La sédimentation lacustre indicateur de changements des paléoenvironnements au cous des 30000 dernières annèes (Carajas, Amazonie, Brésil). *Comptes rendus de l'Académie des sciences* 318: 1645–1652.

Sifeddine A, Martin L, Turcq B, Ribeiro CV, Soubiès F, Cordeiro RC et al. (2001) Variations of the Amazonian rainforest environment: A sedimentological record covering 30,000 years. *Palaeogeography, Palaeoclimatology, Palaeoecology* 168: 221–235.

Snedaker SC (1978) Mangroves: Their value and perpetuation. *Natural Resources* 16: 179–188.

Souza EJ and Pinheiro RVL (2009) *Relações entre as estruturas tectônicas do embasamento e o desenvolvimento da paisagem da região costeira do estado do Amapá uma investigação sobre reativações tectônicas e acumulação de hidrocarbonetos*. Relatório técnico-científico, Brasília: ANP, 105 pp.

Souza Filho PWM, Cohen MCL, Lara RJ, Lessa GC, Koch B and Behling H (2006) Holocene coastal evolution and facies model of the Bragança macrotidal flat on the Amazon mangrove coast, Northern Brazil. *Journal of Coastal Research* SI 39: 306–310.

Szatmari P, Françolin JBL, Zanotto O and Wolff S (1987) Evolução tectônica da margem equatorial brasileira. *Revista Brasileira de Geociências* 17: 180–188.

Thomas RG, Smith DG, Wood JM, Visser J, Calverly-Range EA and Koster EH (1987) Inclined heterolithic stratification: Terminology, description, interpretation and significance. *Sedimentary Geology* 53: 123–179.

Thornton SF and McManus J (1994) Applications of organic carbon and nitrogen stable isotope and C/N ratios as source indicators of organic matter provenance in estuarine systems: Evidence from the Tay Estuary, Scotland. *Estuarine, Coastal and Shelf Science* 38: 219–233.

Toledo MB and Bush MB (2007) A mid-Holocene environmental change in Amazonian savannas. *Journal of Biogeography* 34: 1313–1326.

Tyson RV (1995) *Sedimentary Organic Matter: Organic Facies and Palynofacies*. London: Chapman and Hall, 15 pp.

Vedel V, Behling H, Cohen MCL and Lara RJ (2006) Holocene mangrove dynamics and sea-level changes in Taperebal, northeastern Pará State, northern Brazil. *Vegetation History and Archaeobotany* 15: 115–123.

Van der Hammen T (1974) The Pleistocene changes of vegetation and climate in tropical South America. *Journal of Biogeography* 1: 3–26.

Vinzon BS, Vilela CPX and Pereira LCC (2008) *Processos fisicos na Plataforma Continental Amazônica. Relatório-Técnico, Potenciais Impactos Ambientais do Transporte de Petróleo e Derivados na Zona Costeira Amazônico*. Petrobrás, Brasil, 31 pp.

Walker RG (1992) Facies, facies models and modern stratigrahic concepts. In: Walker RG and James NP (eds) *Facies Models – Response to Sea Level Change*. Ontario: Geological Association of Canada, 1–14.

Walsh GE (1974) Mangroves, a review. In: Reimold RJ and Queens WH (eds) *Ecology of Halophytes*. Academic Press, 51–174.

Weng C, Bush MB and Athens JS (2002) Two histories of climate change and hydrarch succession in Ecuadorian Amazonia. *Review of Palynology and Paleobotany* 120: 73–90.

Wolanski E, Mazda Y, King B and Gay S (1990) Dynamics, flushing and trapping in Hinchinbrook Channel, a giant mangrove swamp, Australia. *Estuarine, Coastal and Shelf Science* 31: 555–579.

Youssef T and Saenger P (1999) Mangrove zonation in Mobbs Bay, Australia. *Estuarine, Coastal and Shelf Science* 49: 43–50.